A carbonate phosphatization model : phosphorites of basal Maquoketa Group (Late Ordovician) of eastern Missouri and eastern Iowa, USA

Autor(en): **Black, Nancy R. / Carozzi, Albert V.**

Objekttyp: **Article**

Zeitschrift: **Archives des sciences et compte rendu des séances de la Société**

Band (Jahr): **41 (1988)**

Heft 2

PDF erstellt am: **17.04.2024**

Persistenter Link: https://doi.org/10.5169/seals-740396

Archs. Sci. Genève	Vol. 41	Fasc. 2	pp. 303-335	1988

A CARBONATE PHOSPHATIZATION MODEL: PHOSPHORITES OF BASAL MAQUOKETA GROUP (LATE ORDOVICIAN) OF EASTERN MISSOURI AND EASTERN IOWA, USA

BY

Nancy R. BLACK and Albert V. CAROZZI[1]

ABSTRACT

A detailed petrographic, mineralogic, and geochemical study was undertaken on 190 samples from four continuous cores cutting across the basal Maquoketa phosphorites in eastern Iowa and Missouri. It shows that a petrographic terminology similar to that of carbonate rocks and based on the grain-size of the principal phosphate fraction and the nature of matrix or cement is indispensable for adequate description and interpretation. Furthermore, a precise definition of phosphorite microfacies requires a combination of petrographic and textural observations with mineralogical determinations of the amounts of calcite, dolomite, apatite, clay minerals, feldspars, quartz, and pyrite, and geochemical determinations of the contents of Ca, Mg, Sr, Fe, and P.

This new combined approach revealed that an assumed simple sequence of phosphorites and associated carbonates and shales consists in reality of sixteen distinct microfacies which build a carbonate-phosphorite depositional model. This model is divided geomorphologically in a landward direction into six different environments: deep basinal, outer slope, bioclastic bar, lower inner slope, upper inner slope, and platform.

The vertical succession of these microfacies indicates a complex cyclicity including two episodes of upwelling and related synsedimentary phosphatization, pyritization, and silicification of upper inner slope and platform carbonates. These conditions are accounted by a simple quasi-geostrophic open ocean model further complicated by glacio-eustatic fluctuations of sea level expressing the late Ordovician glaciation, and local tectonic activity.

A subsequent phase of diagenesis includes evaporite precipitation, calcite cementation, and dolomitization. The latter was extensive in most microfacies, and primarily resulted from a dorag-type freshwater-seawater mixing at the end of the Ordovician.

RÉSUMÉ

Les phosphorites de la base du Groupe Maquoketa ont été étudiées au moyen de 190 coupes minces tirées de quatre sondages entièrement carottés. Cette étude montre que l'analyse et l'interprétation des

[1] Department of Geology, University of Illinois at Urbana-Champaign, Urbana, Illinois, 618011-2999, USA. This paper is part of an MS dissertation completed by NRB under the supervision of AVC.

This research was supported by grants from the Shell Foundation and the Exxon Foundation to the Department of Geology. Gratitude is expressed to Ed Pennington of the Dundee Cement Company and to Brian Witzke of the Iowa Geological Survey for generously providing the four investigated cores.

phosphorites exige l'emploi d'une terminologie pétrographique semblable à celle des carbonates basée sur la taille de la fraction principale phosphatée et sur la nature de la matrice ou du ciment. En outre, une définition précise des microfaciès phosphatés demande la combinaison des caractères pétrographiques et texturaux avec la détermination minéralogique de la teneur en calcite, dolomie, minéraux argileux, feldspaths, quartz et pyrite, et avec la détermination géochimique des teneurs en Ca, Mg, Sr, Fe, et P.

L'application de cette méthodologie montre qu'une série de phosphorites associée avec des carbonates et des shales, en apparence simple, comporte en fait 16 microfaciès différents qui forment un modèle dépositionnel de phosphatisation de carbonates. Ce modèle montre, en direction du continent, les milieux suivants: bassin profond, pente externe, barre bioclastique, pente interne inférieure, pente interne supérieure, et plate-forme.

La succession verticale de ces microfaciès montre une cyclicité complexe comprenant deux épisodes de «upwelling» associés à une phosphatisation, pyritisation et silicification synsédimentaires des sédiments carbonatés de la pente interne supérieure et de la plate-forme. Ces conditions s'expliquent par un modèle simple d'un océan ouvert quasi géostrophique compliqué par des fluctuations glacio-eustatiques du niveau de la mer exprimant la glaciation de la fin de l'Ordovicien, et par les effets d'activités tectoniques locales.

Une phase diagénétique plus tardive comprend la précipitation d'évaporites, une cimentation par la calcite et une dolomitisation. Cette dernière qui s'étend à presque tous les microfaciès résulte de l'effet d'un mélange phréatique d'eau douce et d'eau salée qui s'est produit à la fin de l'Ordovicien.

INTRODUCTION

The Galena-Maquoketa contact (Edenian-Maysvillian) in the upper Mississippi Valley is characterized by a thin, but regionally widespread, phosphatic zone. These phosphorites, at the base of the Maquoketa Group, have been variously interpreted as marking the unconformable to regionally conformable contact with the underlying Galena Group. Drastic changes in the physico-chemical environment of deposition, marked by the basal phosphorites, occurred at the onset of Maquoketa deposition. However, the nature of these changes has not been clearly determined due to the lack of detailed petrographic and diagenetic investigations.

The purpose of this study is to examine in detail the contact between these two formations, to determine what environmental factors were responsible for the drastic change in sedimentation, and to interpret the depositional and diagenetic environments of the basal Maquoketa phosphorites.

STRATIGRAPHY AND PREVIOUS WORK

The literature on the Maquoketa phosphorites microfacies is essentially lithostratigraphic and paleoecological with the exception of the work of Bakush and Carozzi (1986) on the underlying Galena Group which was deposited on an open marine shallow subtidal carbonate ramp. An increase of argillaceous influx during the terminal part of the Galena Group (Dubuque Formation) preceded deposition of shales, argillaceous carbonates, and phosphorites of the basal part of the

Maquoketa Group (Scales Formation) on a subtidal slope and platform morphology which replaced the previous ramp. However, the source areas for argillaceous material in the Dubuque are considered to be local topographic highs along the trend of the Transcontinental Arch whereas the source areas for the Maquoketa shales are considered to be the Taconic terranes to the east (Witzke, 1980, 1983). Unquestionably, the depositional conditions changed abruptly at the Galena-Maquoketa contact but the causes remain disputed.

The currently accepted general interpretation by Brown (1974) postulates that obstruction of normal marine circulation in the epicontinental sea caused by oscillatory rising of the Ozark Dome, was responsible for these changes. Associated with this obstruction of circulation was a periodic upwelling of deep, cold nutrient-rich waters onto the warm shallow carbonate platform, penecontemporaneous submarine replacement of carbonate by marine apatite, and formation of the basal Maquoketa phosphorites. Paleoecological studies of the lower Maquoketa by Bretsky and Bermingham (1970), and Snyder and Bretsky (1971) suggest, however, that the lower Maquoketa underwent large fluctuations in salinity and oxygen levels, as evidenced through faunal and lithologic changes. The faunal assemblage, first described by Ladd (1925) as being composed entirely of unusually small "depauperate" individuals, has been later interpreted as paedomorphic by Snyder and Bretsky (1971) due to the high-stress conditions which have been thought to exist during deposition of the Scales Formation. Kolata and Graese (1983) refined the environmental interpretation of the latter by suggesting that it accumulated in anaerobic to dysaerobic, relatively deep quiet waters, while periodic upwelling by wind-driven currents at the continental margin resulted in synsedimentary phosphatization on the carbonate shelf edge. This periodicity, however, may also relate to tectonic activity associated with the Ozark Uplift, Transcontinental Arch or Wisconsin Arch.

METHODS OF STUDY

Four stratigraphic sections from locations in eastern Iowa and Missouri (Figure 1) were chosen for this study (Black, 1985). Sampling of the four cores included the upper part of the Galena Group (Dubuque Formation), the Galena-Maquoketa contact, and the lower Maquoketa Group, Scales Formation. A total of 190 samples were collected with the sampling interval ranging from 4 cm to 60 cm depending upon the frequency of facies changes observed during macroscopic study of the cores. Petrographic and mineralogic analysis was completed on all samples, and 64 specimens were selected for further chemical analysis.

The thin sections were studied by the microfacies technique described by Bakush and Carozzi (1986). The index of clasticity was determined for all detrital components

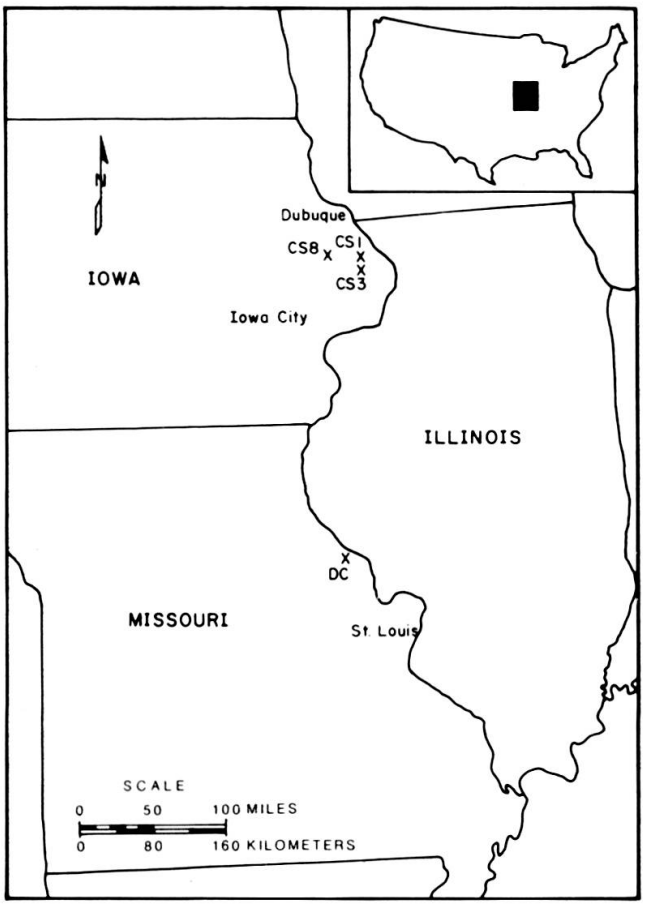

FIG. 1.

Location map of investigated cores. Core sections CS1, CS3 (Jackson County, Iowa) and CS8 (Jones County, Iowa) were obtained from the Iowa Geological Survey and were drilled by Cominco American Incorporated SS-1 Goettler, SS-3 Frost, and SS-8 Welter wells respectively. Core section DC (Jackson County, Missouri) was drilled by the Dundee Cement Company (well 20-74).

including: phosphatic intraclasts, phosphatic lithic pellets, phosphatic ooids, phosphatic spherulites, crinoids, and quartz. Frequency counts were made for the following components: phosphatic intraclasts, phosphatic lithic pellets, phosphatic spherulites, phosphatic ooids, crinoids, quartz, brachiopods, pelecypods, bryozoans, gastropods, trilobites, bone fragments, ostracods, cephalopods, and green algae.

The relative abundance of pyrite, authigenic feldspar and quartz, organic matter, and iron oxide was noted as rare (0 to 1%), present (1 to 5%), common (5 to 15%), and abundant (15 to 100%). In addition, a visual estimate in percentage of matrix, sparite cement, phosphatic components, and remaining components was made.

Whole rock mineralogic data were obtained by X-ray diffraction of powder samples. Atomic absorption spectroscopy (for determination of Fe, Mg, Ca, and Sr) and colorimetric spectrophotometry (for determination of P) were performed on selected samples of the various microfacies. Detailed description of these techniques are found in Black (1985).

COMPONENTS AND TERMINOLOGY

The boundary between matrix and components was set at 60 μm for both skeletal material and inorganic debris, because below this size no identification is possible with a petrographic microscope. Dolomitization, resulting in extensive replacement and recrystallization, often made identification of biogenic components difficult, and limited to morphology alone.

The major organic components observed include: crinoids, brachiopods, cephalopods, trilobites, and ostracods. Minor organic components include: gastropods and pelecypods, bryozoans, dasyclads, bone fragments, and phosphatic spherulites. Phosphatic spherulites are defined as tiny grains (50-100 μm) which are spherical or slightly ellipsoidal in shape, have no internal structure, and are extremely well-rounded. They are considered to be organic in origin, possibly fecal, due to their extreme regularity of shape, and clear distinction, in size and crystallinity, from lithic pellets.

The inorganic components are quartz, phosphatic lithic pellets, phosphatic intraclasts, phosphatic ooids, and phosphatic nodules. Angular, silt-size quartz is present, but due to the difficulties in counting the fine grains (often <0.08 mm), the X-ray data for quartz are considered a more reliable indicator of its occurrence. The pellets are interpreted as lithic in origin, and are elongated or ellipsoidal (length to width ratio = 2: 1) phosphatic particles with no apparent internal structure. They are, for the most part, poorly crystalline apatite, ranging in size from 0.05 to 0.5 mm. Intraclasts are the intraformationally reworked fragments of usually weakly consolidated phosphatic sediment. These intraclasts are usually moderately well rounded with somewhat irregular shapes, and often contain particles (bioclasts, pellets, etc.) within, and range in size from 0.1 to greater than 3 mm. Ooids and superficial ooids vary in shape from spherical to highly ellipsoidal and deformed. Composite ooids are common. Often no nucleus is apparent (probably due to penecontemporaneous replacement by apatite), and the size ranges from 0.1 to 2 mm. Phosphatic nodules consist of aggregates of particles agglutinated by phosphatic cement and characterized by very irregular boundaries. It is often difficult to distinguish nodules from intraclasts, but if it appears that the particle has been formed *in situ,* it is considered a nodule.

The petrographic classification of marine phosphorites used in this study is modified from Slansky (1980) and is similar to that of carbonate rocks. It utilizes two basic parameters: grain-size of the predominant ($>10\%$) phosphatic figured constituents, and nature of matrix or cement. Phosphalutite (0.01 to 0.03 mm), phosphasiltite (0.03 to 0.064 mm), phospharenite (0.064 to 2 mm), and phospharudite (>2 mm) are further qualified by prefixes such as bio-, pel-, oo-, intra-, extra-, to describe bioclasts, pellets, ooids, intraclasts and extraclasts.

Phosphalutites and phosphasiltites may contain up to 10 percent sand-size components of organic or inorganic origin. Phospharenites containing 10 to 30 percent sand-size constituents in a matrix of phosphalutite or phosphasiltite are called matrix-supported, those with more than 30 percent sand-size constituents and possessing an interstitial matrix as above or a cement of precipitated collophanite (microsphatite <0.01 mm) are called grain-supported. Non-phosphatic constituents which may form part of the matrix (quartz, glauconite, clay minerals) or part of the cement (carbonates, silica) are designated according to their mineralogy, grain- or crystal-size, and relative abundance, such as: grain-supported oophospharenite with 10 percent quartz-glauconite matrix, or grain-supported pelphospharenite with 20 percent sparite cement. Phospharudites contain more than 30 percent granule- (2 to 4 mm) or pebble- (4 to 64 mm) size constituents with interstitial material of all previous phosphatic types.

DESCRIPTION OF MICROFACIES

Petrographic and X-ray diffraction study showed the existence of 16 distinct dolomitized microfacies which can be divided into a carbonate sequence (microfacies 1 to 11) and a phosphorite sequence (microfacies 12 to 16). These two sequences are associated in a carbonate-phosphorite depositional model (to be discussed later) divided, geomorphologically in a landward direction, in six different environments: basin, outer slope, bioclastic bar, lower inner slope, upper inner slope, and platform. The various microfacies are described in this general shallowing-upward order. However, it should be pointed out that microfacies 12 to 16 are approximate depositional equivalents to microfacies 8 to 11 in terms of relative position to shoreline and energy, but differ in their early diagenetic chemical environment which corresponded to phosphatization by upwelling.

Basin

Microfacies 1 (Plate 1A)

Dolomitized (40 to 100%) calcareous bituminous shale interbedded with calcisiltite laminae. Minute flattened ostracods, phosphatic pellets and spherulites, and occasional sparite-filled trilobites are associated with the calcisiltite stringers. Pyritized organic debris, pyrite rhombs, and euhedral rhombs of dolomite are pervasive.

Average mineral composition is in %: 5 calcite, 22 dolomite, 19 quartz, 3 potassium feldspar, 33 clay minerals, 5 apatite, 13 pyrite. Elemental averages are: Ca 66×10^3 ppm, Sr 125 ppm, Fe 24×10^3 ppm, Mg 34×10^3 ppm, and P 6×10^3 ppm.

Microfacies 1A is a non-dolomitized variety which contains calcite pseudomorphs after nodular anhydrite.

Microfacies 2 (Plate 1B)

Dolomitized (100%) calcareous mudstone with less than 10 percent scattered, well-rounded phosphatic intraclasts and pellets. Rare brachiopod and cephalopod fragments (replaced by apatite) are present. Scattered pyritized organic matter is common in the groundmass which displays abundant equant dolomite rhombs.

Average mineral composition is in %: 31 dolomite, 9 quartz, 2 potassium feldspar, 44 clay minerals, 5 apatite, 9 pyrite. Elemental averages are: Ca 83×10^3 ppm, Sr 114 ppm, Fe 24×10^3 ppm, Mg 56×10^3 ppm, and P 0.8×10^3 ppm.

Outer Slope

Microfacies 3 (Plate 1C)

Dolomitized (100%) argillaceous biomicrite with less than 10 percent scattered bioclasts of crinoids, ostracods, cephalopods, and brachiopods, phosphatic lithic pellets, and intraclasts. Brachiopods and ostracods are commonly replaced by pyrite, but the latter occurs also as a replacement of other scattered minute organic debris. Bioturbation is common and represented by well-defined burrows characterized by larger dolomite rhombs and concentrations of pyritized and phosphatic constituents. Average mineral composition is in %: 48 dolomite, 10 quartz, 2 potassium feldspar, 29 clay minerals, 2 apatite, 9 pyrite. Elemental averages are: Ca 138×10^3 ppm, Sr 115 ppm, Fe 20×10^3 ppm, Mg 62×10^3 ppm, and P 4×10^3 ppm.

Microfacies 4 (Plate 1D)

Dolomitized (100%) argillaceous biocalcisiltite with 10 percent scattered sand-size bioclasts of ostracods and brachiopods predominant over crinoids, cephalopods, and pelecypods. Large, thin ostracods are often silicified, cephalopod fragments replaced by apatite, whereas brachiopod and pelecypod bioclasts are replaced by dolosparite. Phosphatic pellets, spherulites, and rare intraclasts are concentrated in burrows and circular arrangements due to bioturbation.

Average mineral composition is in %: 47 dolomite, 10 quartz, 2 potassium feldspar, 26 clay minerals, 6 apatite, 9 pyrite. Elemental averages are: Ca 161×10^3 ppm, Sr 145 ppm, Fe 20×10^3 ppm, Mg 83×10^3 ppm, and P 7×10^3 ppm.

Bioclastic Bar

Microfacies 5 (Plate 1E)

Dolomitized (100%) matrix-supported biocalcarenite with argillaceous calcilutite to calcisiltite matrix. Bioclasts reach 20 percent and consist mostly of

crinoids, brachiopods, and trilobites with lesser amounts of ostracods, phosphatic spherulites, and intraclasts. Bioclasts if not pyritized or silicified, are replaced by dolosparite. Marginal replacement of silicified crinoid fragments by dolomite rhombs indicates silicification preceded dolomitization. Bioturbation gives a mottled texture to the matrix.

Average mineral composition is in %: 56 dolomite, 10 quartz, 1 potassium feldspar, 22 clay minerals, 4 apatite, 7 pyrite. Elemental averages are: Ca 157×10^3 ppm, Sr 141 ppm, Fe 22×10^3 ppm, Mg 88×10^3 ppm, and P 5×10^3 ppm.

Microfacies 6 (Plate 1F)

Dolomitized (100%) grain-supported biocalcarenite with argillaceous calcilutite to calcisiltite matrix. Trilobite and brachiopod bioclasts predominate over crinoids. All bioclasts are either pyritized or replaced by dolosparite. Poorly crystalline and organic-rich phosphatic pellets and intraclasts are present in moderate amounts. Coarser dolomite crystals are concentrated in burrows.

PLATE 1.

Typical microfacies of Maquoketa phosphorites.

A. Microfacies 1: Dolomitized (100%) bituminous calcareous shale with interbedded stringers of calcisiltite. Pyrite occurs as rhombs and disseminated flakes.

B. Microfacies 2: Dolomitized (100%) calcareous mudstone with less than 10 percent scattered phosphatic intraclasts and lithic pellets. Pyritized organic debris are common. Bioturbation has produced this mottled texture.

C. Microfacies 3: Dolomitized (100%) argillaceous biomicrite with less than 10 percent scattered bioclasts, phosphatic lithic pellets and intraclasts. Well-defined burrows are characterized by larger dolomite rhomb size and pyritized organic debris.

D. Microfacies 4: Dolomitized (100%) argillaceous biocalcisiltite with scattered sand-size bioclasts. Ostracods (center right) and brachiopods are predominant.

E. Microfacies 5: Dolomitized (100%) matrix-supported biocalcarenite with argillaceous calcisiltite matrix. Scattered crinoids are replaced by dolomite, but retain much of their original structure (upper right), often bioclasts are silicified (center).

F. Microfacies 6: Dolomitized (100%) grain-supported biocalcarenite with argillaceous calcilutite matrix. Brachiopods, trilobites, and pelecypods are replaced by dolosparite. Poorly crystalline and highly organic phosphatic intraclasts and pellets are present.

G. Microfacies 7: Dolomitized (100%) organic matter-rich biomicrite. Heavy bioturbation resulted in a patchy microsparite cement.

H. Microfacies 8: Dolomitized (100%) biocalcisiltite with up to 10 percent sand-size bioclasts. Scattered crinoid fragments, and a few silicified bioclasts predominate.

All photomicrographs: plane-polarized light.

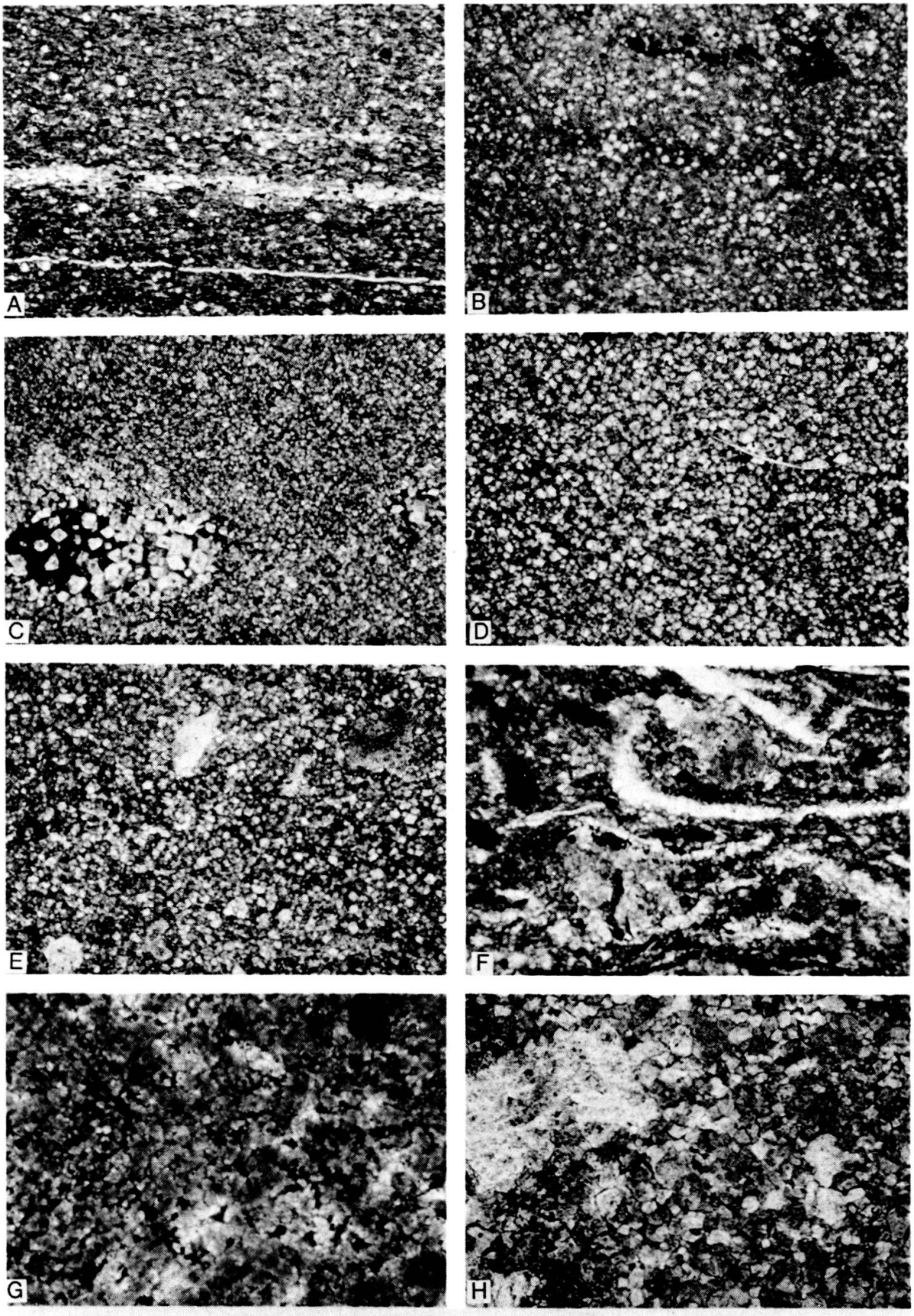
A
B
C
D
E
F
G
H
0.5mm

Average mineral composition is in %: 71 dolomite, 5 quartz, 1 potassium feldspar, 16 clay minerals, 3 apatite, 4 pyrite. Elemental averages are: Ca 156×10^3 ppm, Sr 185 ppm, Fe 21×10^3 ppm, Mg 93×10^3 ppm, and P 0.6×10^3 ppm.

Lower Inner Slope

Microfacies 7 (Plate 1G)

Dolomitized (100%) organic-matter rich biomicrite with less than 10 percent sand-size bioclasts with scattered small patches of microsparite cement due to intense bioturbation. The next frequent bioclasts are micritized crinoids associated with lesser amounts of brachiopods and bone fragments. Disseminated pyrite pigments and nodules are abundant.

Average mineral composition is in %: 73 dolomite, 2 quartz, 5 clay minerals, 5 apatite, 15 pyrite. Elemental averages are: Ca 131×10^3 ppm, Sr 73 ppm, Fe 132×10^3 ppm, Mg 86×10^3 ppm, and P 0.2×10^3 ppm.

Microfacies 8 (Plate 1H)

Dolomitized (100%) biocalcisiltite with up to 10 percent scattered sand-size bioclasts which are mostly crinoids associated with lesser amounts of brachiopods, bone fragments, and phosphatic intraclasts. Bioturbation is extensive leading to a mottled texture. Dolomitization which displays cloudy-centered rhombs often with rims of ferroan dolomite was preceded by partial replacement of crinoids and brachiopods by silica, and a patchy replacement by phosphates related to bioturbation.

Average mineral composition is in %: 82 dolomite, 5 quartz, traces of potassium feldspar, 7 clay minerals, 3 apatite, 3 pyrite. Elemental averages are: Ca 206×10^3 ppm, Sr 55 ppm, Fe 11×10^3 ppm, Mg 123×10^3 ppm, and P 0.8×10^3 ppm.

Upper Inner Slope

Microfacies 9 (Plate 2A)

Dolomitized (100%) matrix-supported biocalcarenite with calcisiltite matrix and up to 30 percent sand-size bioclasts. Crinoids and brachiopods predominate over bone fragments, phosphatic intraclasts, and lithic pellets. Most bioclasts are replaced by dolosparite, except where silicification or phosphatization has occurred previously. Phosphatic constituents are concentrated within and around the frequent burrows due to bioturbation which correspond to patches of coarser and clear dolomite rhombs.

Average mineral composition is in %: 91 dolomite, 2 quartz, traces of potassium feldspar, 5 clay minerals, 2 apatite. Elemental averages are: Ca 235×10^3 ppm, Sr 109 ppm, Fe 7×10^3 ppm, Mg 92×10^3 ppm, and P 3×10^3 ppm.

Microfacies 10 (Plate 2B)

Dolomitized (100%) matrix-to grain-supported biocalcarenite with scattered phosphatic ooids, pellets, and intraclasts in a bioturbated calcisiltite matrix with patches of interparticle sparite cement. Bioclasts of crinoids, trilobites, brachiopods predominate over cephalopods; replacement is either by dolosparite or apatite. Bioturbation leads to a patchy replacement of the matrix by microcrystalline apatite and concentration of the phosphatic ooids and pellets reworked from microfacies 12 to 16.

Average mineral composition is in %: 75 dolomite, 3 quartz, traces of potassium feldspar, 7 clay minerals, 9 apatite, 6 pyrite. Elemental averages are: Ca 232×10^3 ppm, Sr 215 ppm, Fe 13×10^3 ppm, Mg 65×10^3 ppm, and P 22×10^3 ppm.

Microfacies 11 (Plate 2C)

Dolomitized (100%) grain-supported biocalcarenite with calcisiltite matrix and patchy sparite cement. Crinoid and brachiopod bioclasts predominate over trilobites and ostracods; replacement is either by dolosparite, apatite, or silica. Bioturbation concentrated phosphatic lithic pellets and intraclasts and irregularly distributed the various bioclasts. Silicification of brachiopod and crinoid fragments preceded dolomitization.

Average mineral composition is in %: 91 dolomite, 2 quartz, 5 clay minerals, 2 apatite. Elemental averages are: Ca 200×10^3 ppm, Sr 213 ppm, Fe 2×10^3 ppm, Mg 90×10^3 ppm, and P 1×10^3 ppm.

Phosphatized Upper Inner Slope

Microfacies 12 (Plate 2D)

Dolomitized (100%) matrix-to grain-supported intraclastic oolitic pelphospharenite with an argillaceous calcisiltite matrix and patches of interparticle sparite cement. Bioclasts of cephalopods and brachiopods are replaced by apatite and silica, and silicified ostracods are filled by phosphalutite. Phosphatic ooids and pellets are associated with intraclasts of phosphalutite and phosphasiltite containing themselves ooids, lithic pellets, bioclasts, and minute grains of detrital quartz and feldspar. The heterogeneous distribution of the components indicates widespread bioturbation. Patchy phosphatization of the matrix by microcrystalline apatite preceded dolomitization.

Average mineral composition is in %: 37 dolomite, 7 quartz, 1 potassium feldspar, 19 clay minerals, 30 apatite, 6 pyrite. Elemental averages are: Ca 246×10^3 ppm, Sr 633 ppm, Fe 18×10^3 ppm, Mg 40×10^3 ppm, and P 71×10^3 ppm.

Microfacies 13 (Plate 2E)

Dolomitized (100%) grain-supported intraclastic oolitic pelphospharenite to phospharudite with argillaceous calcisiltite matrix and patches of sparite cement. Phosphatic intraclasts, ooids, and lithic pellets with abundant apatite-replaced orthocone cephalopods and brachiopods predominate over large silicified ostracods filled with phosphalutite. Partial phosphatization of the matrix developed a few nodules while subsequent dolomitization partially replaced phosphatic intraclasts and pellets. Nodular and disseminated pyrite is ubiquitous.

Average mineral composition is in %: 26 dolomite, 5 quartz, 1 potassium feldspar, 9 clay minerals, 45 apatite, 14 pyrite. Elemental averages are: Ca 251×10^3 ppm, Sr 601 ppm, Fe 44×10^3 ppm, Mg 27×10^3 ppm, and P 89×10^3 ppm.

PLATE 2.

Typical microfacies of Maquoketa phosphorites *(continued)*.

A. Microfacies 9. Dolomitized (100%) matrix-supported biocalcarenite with calcisiltite matrix. Crinoid fragments are common. Bioturbation is indicated by mottled texture and patches of coarser clear dolomite rhombs.

B. Microfacies 10. Dolomitized (100%) matrix- to grain-supported biocalcarenite with scattered phosphatic ooids, lithic pellets and intraclasts in a calcisiltite matrix with patches of interparticle sparite cement. Phosphatic pellets and ooids are concentrated in patches resulting from bioturbation.

C. Microfacies 11. Dolomitized (100%) grain-supported biocalcarenite with calcisiltite matrix and patchy sparite cement. Crinoid fragments are moderately well preserved.

D. Microfacies 12: Dolomitized (100%) matrix- to grain-supported intraclastic oolitic pelphospharenite with argillaceous calcisiltite matrix and patchy sparite cement. Bioturbation causes irregular distribution of components. Pellets and ooids are variable in size but regular in shape.

E. Microfacies 13: Dolomitized (100%) grain-supported intraclastic oolitic pelphospharenite to phospharudite with argillaceous calcisiltite matrix and patches of sparite cement. In this particular sample, the matrix is an oolitic pelphospharenite with argillaceous calcisiltite matrix. Phosphalutite-filled ostracods and orthocone cephalopods (center) are common. Disseminated pyrite is abundant.

F. Microfacies 14: Dolomitized (100%) grain-supported to pressure-welded intraclastic pelletoidal oophospharenite to phospharudite with argillaceous calcisiltite matrix and sparite cement. Dolomite has partially replaced some grains. Many ooids are highly deformed by compaction.

G. Microfacies 15: Dolomitized (100%) pressure-welded intraclastic oolitic biophospharenite with sparite cement. Phosphatic nodules (upper left) are common.

H. Microfacies 16: Dolomitized (100%) nodular intraphospharudite with pelletoidal oophospharenite matrix and a patchy microsparite cement. Organic matter content is high. Intraclasts contain phosphatic pellets and ooids.

All photomicrographs: plane-polarized light.

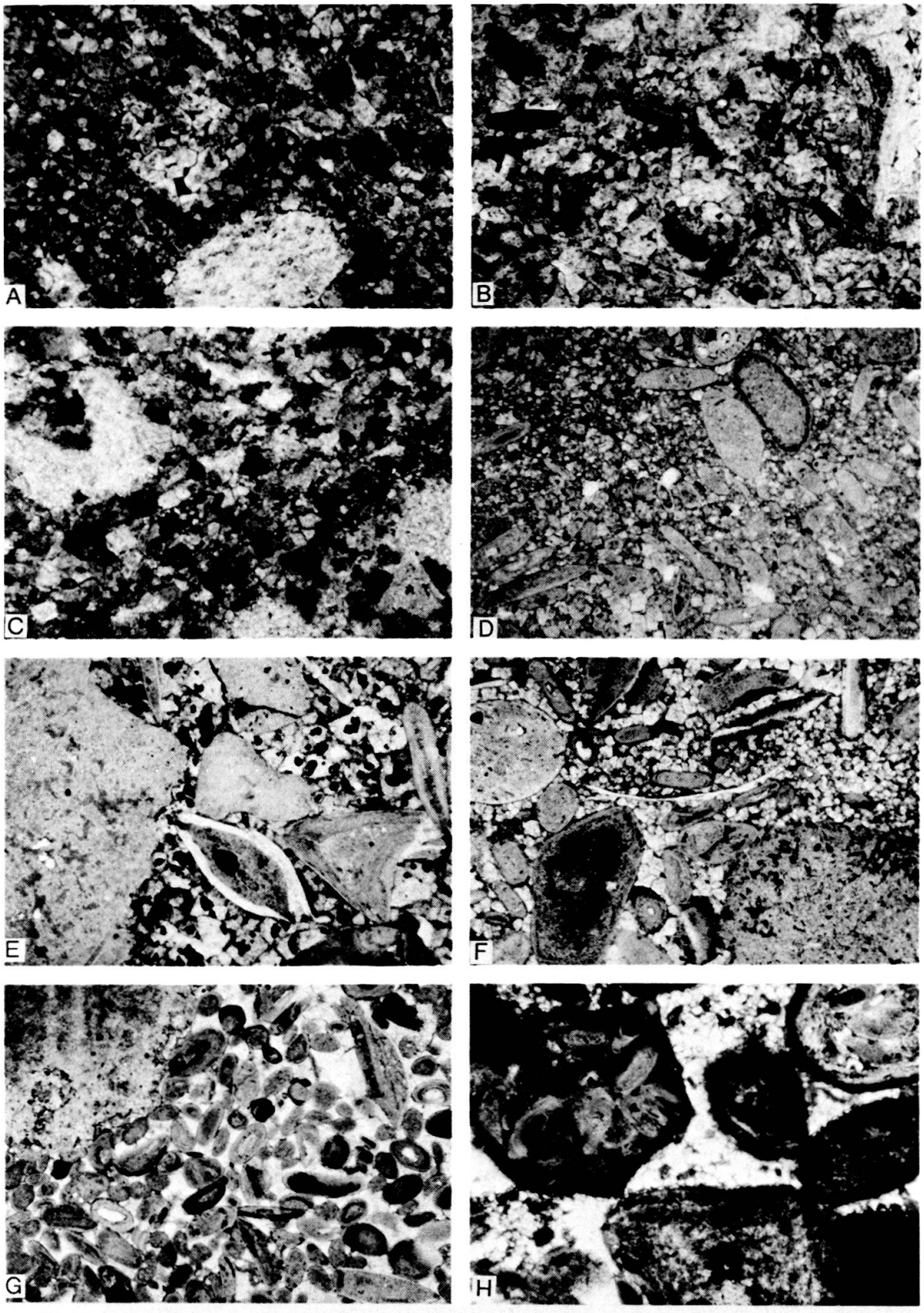
A
B
C
D
E
F
G
H
0.5mm

Microfacies 14 (Plate 2F)

Dolomitized (100%) grain-supported to pressure-welded intraclastic pelletoidal oophospharenite to phospharudite with argillaceous calcisiltite matrix and patches of sparite cement. Phosphatic intraclasts, ooids, and lithic pellets predominate over lesser amounts of cephalopods, brachiopods, and large ostracods. Bioclasts are either replaced by apatite or silica. Early phosphatization generated large nodules also whereas late dolomitization replaced the original matrix and cement, and the margins of phosphatic grains and nodules. Pyrite replacement of grains and matrix is also common.

Average mineral composition is in %: 37 dolomite, 3 quartz, traces of potassium feldspar, 12 clay minerals, 44 apatite, 4 pyrite. Elemental averages are: Ca 213×10^3 ppm, Sr 348 ppm, Fe 14×10^3 ppm, Mg 75×10^3 ppm, and P 58×10^3 ppm.

Phosphatized Platform

Microfacies 15 (Plate 2G)

Dolomitized (100%) pressure-welded intraclastic oolitic biophospharenite with sparite cement. Phosphatic ooids, pellets, and intraclasts of oolitic biophospharenite are abundant. The most frequent bioclasts are apatite-replaced cephalopods and brachiopods together with silicified ostracods filled with phosphalutite. Pyrite replacement of phosphatic grains and orthocone cephalopods is common. Subsequent dolomitization led to partial replacement of apatite grains and of original interparticle sparite cement by a mosaic of dolosparite.

Average mineral composition is in %: 19 dolomite, 1 quartz, traces of potassium feldspar, 3 clay minerals, 60 apatite, 17 pyrite. Elemental averages are: Ca 240×10^3 ppm, Sr 732 ppm, Fe 36×10^3 ppm, Mg 32×10^3 ppm, and P 95×10^3 ppm.

Microfacies 16 (Plate 2H)

Dolomitized (100%) nodular intraphospharudite with pelletoidal oophospharenite matrix and patchy sparite cement. Besides large nodules due to replacement of the matrix by apatite, phosphatic intraclasts predominate and consist of phosphatic ooids, pellets, brachiopods, and other bioclasts set in a phosphalutite matrix very rich in organic matter. Isolated bioclasts of brachiopods and ostracods are scattered in the interstitial material which can be replaced locally by masses of pyrite. Subsequent dolomitization also marginally replaced all phosphatic constituents besides original matrix and cement.

Average mineral composition is in %: 23 dolomite, 4 quartz, 1 potassium feldspar, 7 clay minerals, 51 apatite, 14 pyrite. Elemental averages are: Ca 255×10^3 ppm, Sr 429 ppm, Fe 25×10^3 ppm, Mg 32×10^3 ppm, and P 106×10^3 ppm.

VERTICAL EVOLUTION OF DEPOSITIONAL ENVIRONMENTS

The described microfacies of the uppermost Galena and lower Maquoketa were deposited in a number of different environments ranging from deep restricted basin to a shallow, high energy platform. This large fluctuation in environmental conditions was presumably the result of a combination of glacio-eustatic fluctuations of sea level combined with local tectonic activity in the region to be discussed later.

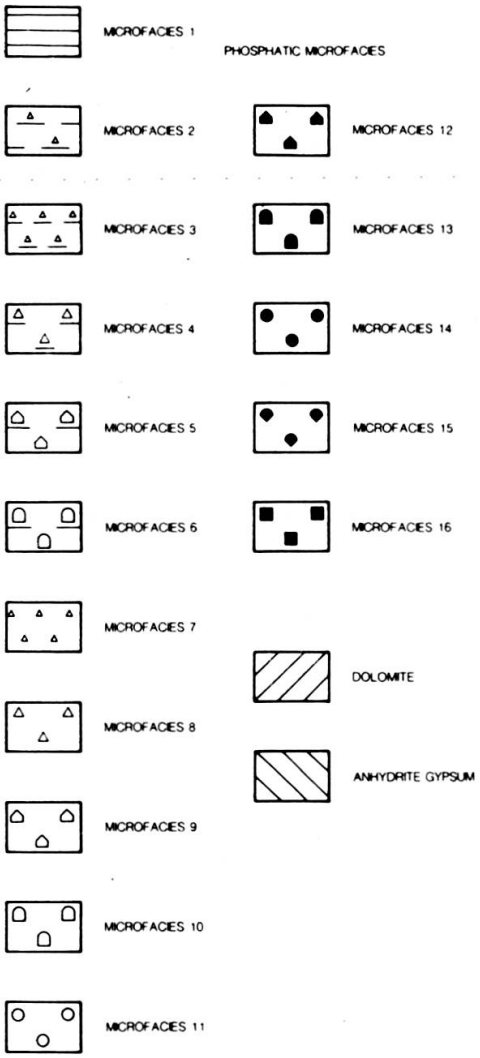

FIG. 2.

Symbols for microfacies.

The four investigated cores (Black, 1985) are essentially similar and the core of well CS8 is used as a typical example (Figures 2, 3, 4). Variations of organic and inorganic components, and of mineralogical and chemical data are graphically illustrated from left to right as follows: column of microfacies (refer to Figure 2 for symbols) with a depth scale in meters and location of samples or control points; graphic illustration of the major textural features in percent surface area; mineralogical parameters as determined through X-ray diffraction in percent; chemical parameters as determined through atomic absorption spectroscopy and spectrophotometry in ppm; variation curves of the frequency and clasticity of inorganic components, and the frequency of organic components; an environmental interpretation curve which expresses the relative position of the various microfacies in terms of bathymetry and morphology of the sea floor.

The sequence of environments represented by core CS 8 is expressed by the superposition of 6 events or phases (Figures 3, 4).

Phase 1

Shallowing-upward sequence from lower inner slope to upper inner slope, that is microfacies 7 to 11 (uppermost Galena).

Crinoids, brachiopods, and scattered bone fragments are associated with a small amount of phosphatic intraclasts, pellets, and ooids transported from adjacent parts of the basin. Calcium, magnesium, and strontium contents are fairly constant, but fluctuate slightly with varying calcite or dolomite percentages. Phosphorus is low and iron varies slightly except in microfacies 7 where locally restricting conditions have allowed for accumulation of organic matter and subsequent precipitation of pyrite. In general, these carbonates were deposited under normal marine conditions.

Phase 2

Phosphatization by upwelling of the upper inner slope and platform with formation of microfacies 12 to 16 (phosphorites of Galena-Maquoketa contact). These phospharenites are characterized by an abundance of siliceous ostracods and phosphatized cephalopods, and a gradual decrease (upsection) of crinoids and brachiopods. Phosphatic nodules, intraclasts, pellets, and ooids are predominant. Upwelling conditions produce modifications in the chemical content of the sediments including an increase in P, Ca, Sr, and Fe, while Mg content decreases significantly. The variations in Ca, Fe, and P correspond directly with mineralogical variations, whereas the Sr content indicates additional concentration in apatite and total Mg (possibly reflecting the Mg content of interstitial waters at the time of deposition) varies inversely with calcium. The conditions necessary for the observed trends are those required for phosphatization: an increase in temperature, accumulation of organic matter, and reduction of pH.

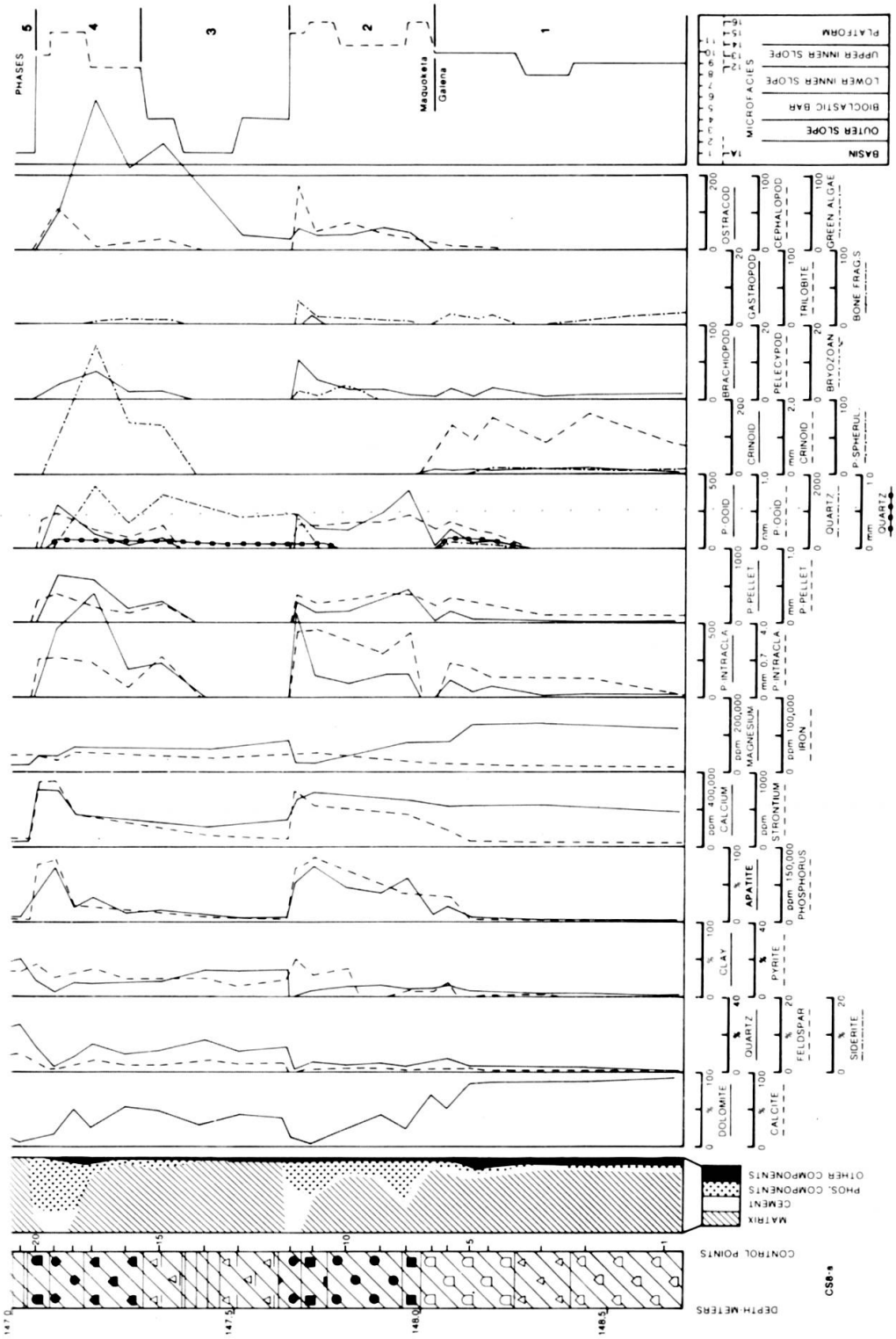

FIG. 3.

Typical example of vertical variation of microscopic and chemical parameters in core CS8.

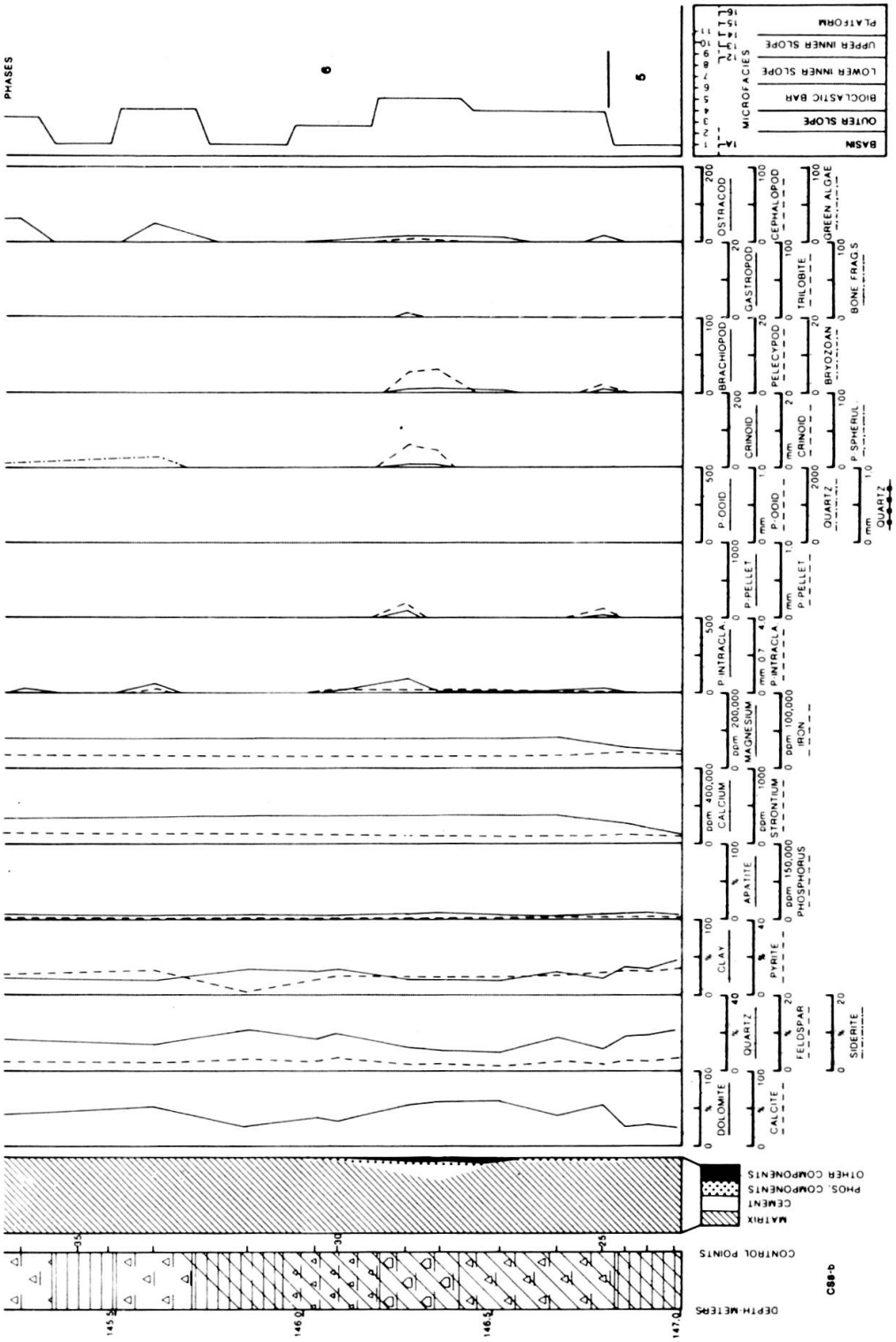

FIG. 4.

Typical example of vertical variation of microscopic and chemical parameters in core CS8 *(continued)*.

Phase 3

Rapid deepening down to basin and outer slope with microfacies 1 to 4 and equally rapid shallowing-upward back to upper inner slope (Lower Maquoketa). Few organic (graptolites and ostracods are the exception) and inorganic components are present in these generally reducing conditions. Strontium and calcium content decrease with the decrease in carbonate deposition, while magnesium increases and iron remains fairly constant.

Phase 4

Phosphatisation by upwelling of the upper inner slope with formation of microfacies 12 to 14 and concentration of phosphatic grains by reworking (Lower Maquoketa).

This second phase of phosphatization is similar to, but shorter than the first with regard to the distribution of organic and inorganic components, mineralogy, and chemistry.

Phase 5

Rapid deepening down to basinal conditions with microfacies 1 (Lower Maquoketa), with low calcium, strontium and phosphorus characteristic of bituminous shales deposited in a quiet low oxygen environment.

Phase 6

Shallowing-upward sequence with several oscillations from basinal conditions to bioclastic bar that is microfacies 1 to 6 (Lower Maquoketa), deposited below wave base but in a well-oxygenated environment.

The above-mentioned environmental evolution which is common to the four investigated cores can be represented graphically by an ideal shallowing-upward sequence (Figure 5). This sequence consists of the carbonate suite of microfacies 1 through 11 and its partial overlap in the upper inner slope and platform environments (microfacies 8 to 11) by the phosphatic suite of microfacies 12 through 16. Next to the microfacies column are drafted curves representing the variation of averages of clasticity and frequency of components, averages of chemical and X-ray parameters, averages of dolomite crystal size, and percent surface area for matrix, cement, phosphatic and non-phosphatic (other) components.

The heavier, bolder lines represent data from microfacies 12 through 16, while the lighter lines represent data from microfacies 1 through 11. For ease of comparison between phosphatic and non-phosphatic microfacies, some of the scales of components in microfacies 12 to 16 have been offset to avoid excessive overlap of data points.

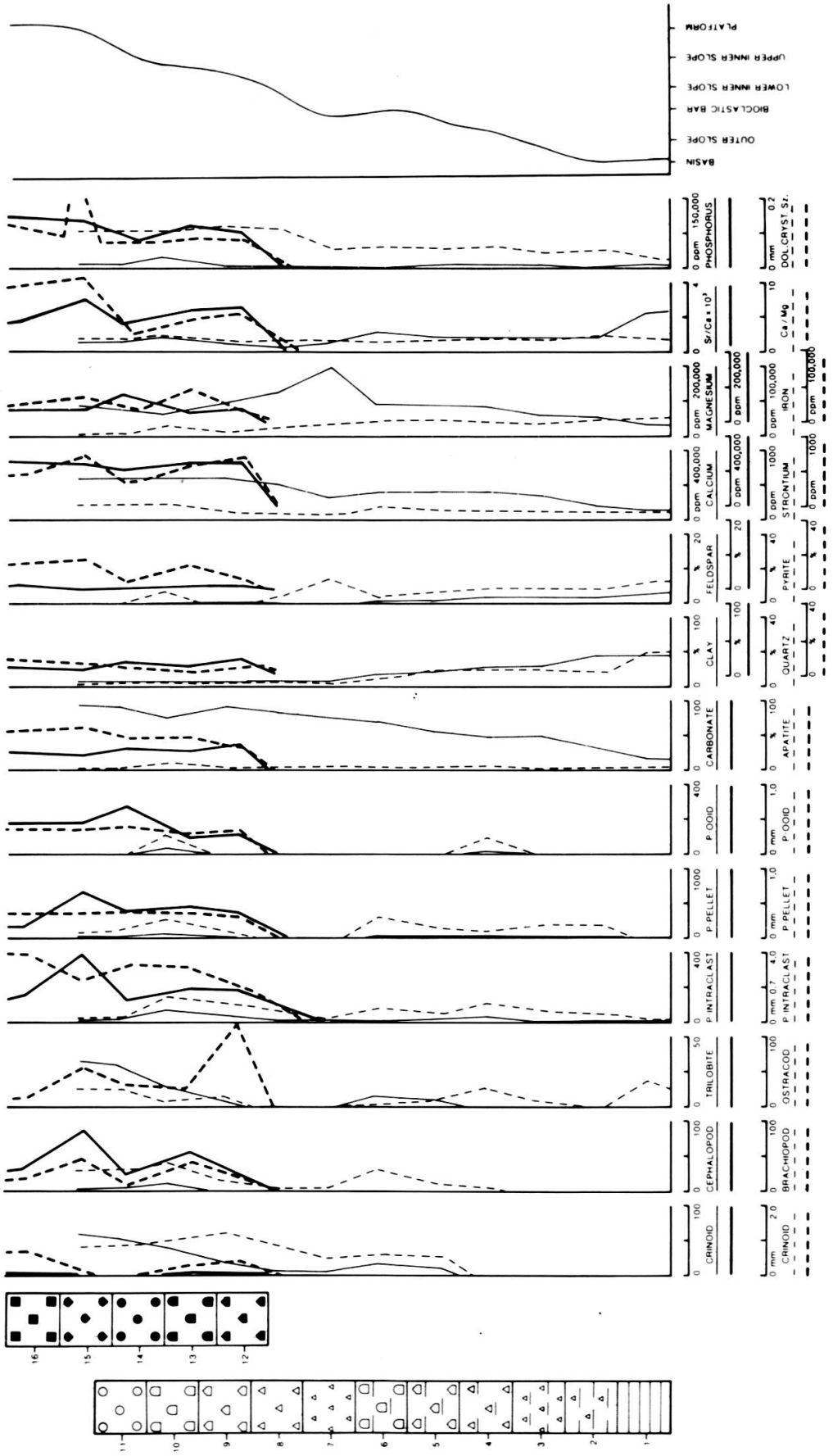

FIG. 5. Ideal shallowing-upward sequence.

Practically, the ideal shallowing-upward sequence is more conveniently discussed, in a genetic viewpoint when transformed according to Walther's rule into a horizontal ideal depositional model which shows the variations of all constituents in the context of submarine morphology.

IDEAL DEPOSITIONAL MODEL

In the proposed model (Figures 6, 7), with the exception of the platform microfacies, the sediments were deposited almost *in situ* or by fairly weak bottom currents both down slope and upward. The presence of weak currents along the slope is indicated by the change in depositional conditions from microfacies 8 through 11 to microfacies 12 through 16. The highest frequency of crinoids occurs in microfacies 10 and 11, and generally decreases seaward indicating that crinoid colonies mainly existed on the platform and that only minor colonies of smaller crinoids lived under slope conditions with a slightly higher frequency in association with the bioclastic bar. Few crinoids are present in microfacies 12 through 16 due to their apparent intolerance for unfavorable physico-chemical conditions which resulted in the synsedimentary phosphatization of platform carbonates.

The frequency curve of brachiopods generally mimics that of crinoids; brachiopods participate appreciably in the generation of the bioclastic bar. They increase in frequency in microfacies 12 through 16 indicating a greater tolerance than crinoids for synsedimentary phosphatization. Orthocone cephalopods represent the predominant fraction of bioclasts in microfacies 12 through 16. This occurrence indicates that they were either autochthonous platform dwellers during phosphatization or that they were brought in by weak bottom currents and concentrated mechanically in a greater energy microfacies. A nearshore and an offshore population of ostracods is clearly displayed, and their peak of frequency in microfacies 12 on the edge of the area of synsedimentary phosphatization may represent a mechanical concentration by weak bottom currents. Trilobite frequency is greatest in microfacies 11 (platform edge) and decreases seaward with a second increase associated with the bioclastic bar. This pattern is expected of scavengers in relation to other peaks of benthic constituents such as crinoids and brachiopods.

Most of the phosphatic constituents were generated in upper inner slope to platform conditions (microfacies 12 through 16) as shown by the behavior of phosphatic intraclasts, phosphatic pellets derived from their disintegration, phosphatic ooids, and phosphatic spherulites of fecal origin. Weak bottom currents transported seaward a reduced number of the smaller phosphatic constituents which occasionally were concentrated in the bioclastic bar.

The overall greater matrix content and the very small cement content of the basin, outer slope, and lower inner slope environments are indicative of general low energy

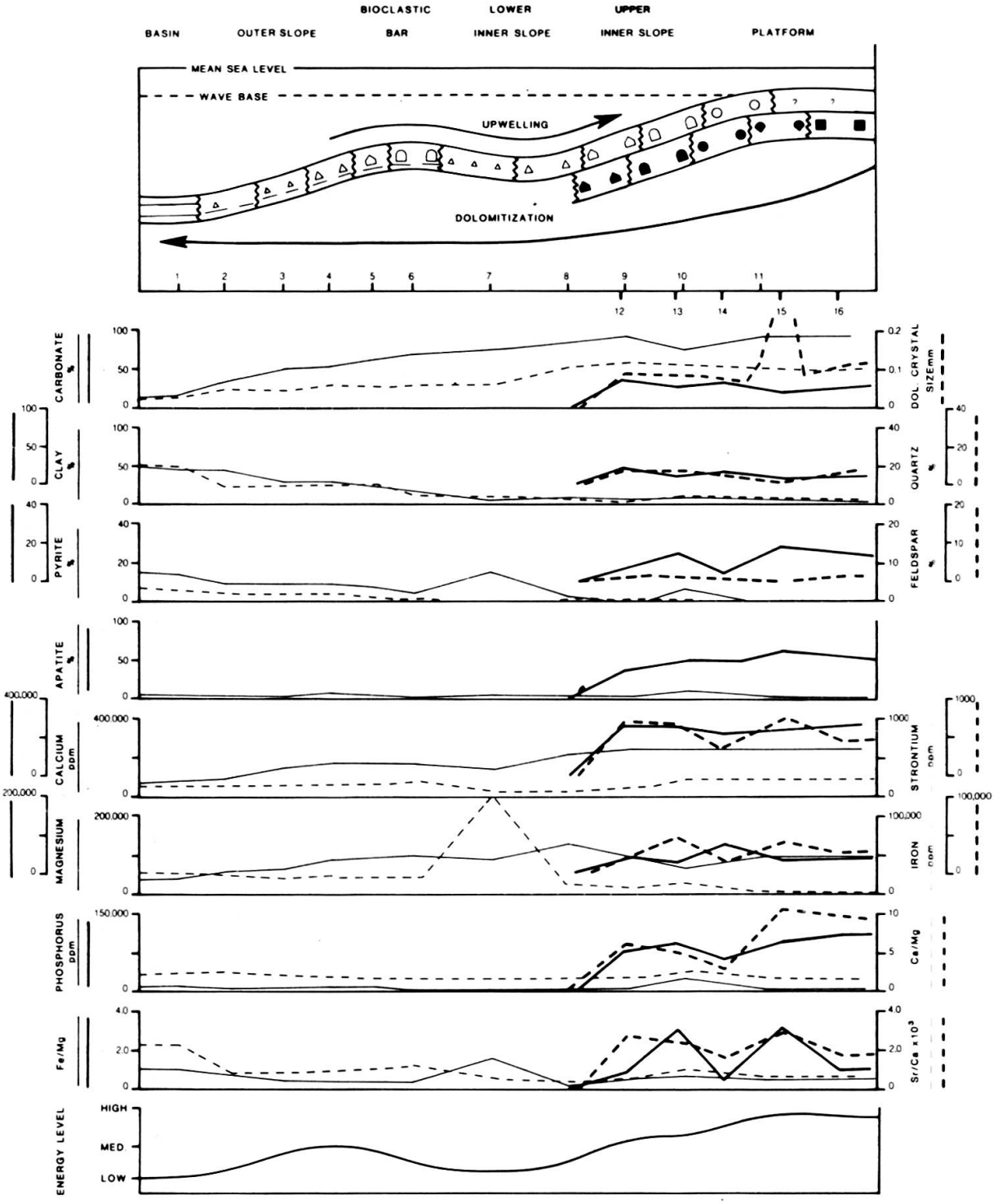

FIG. 6.

Ideal depositional model.

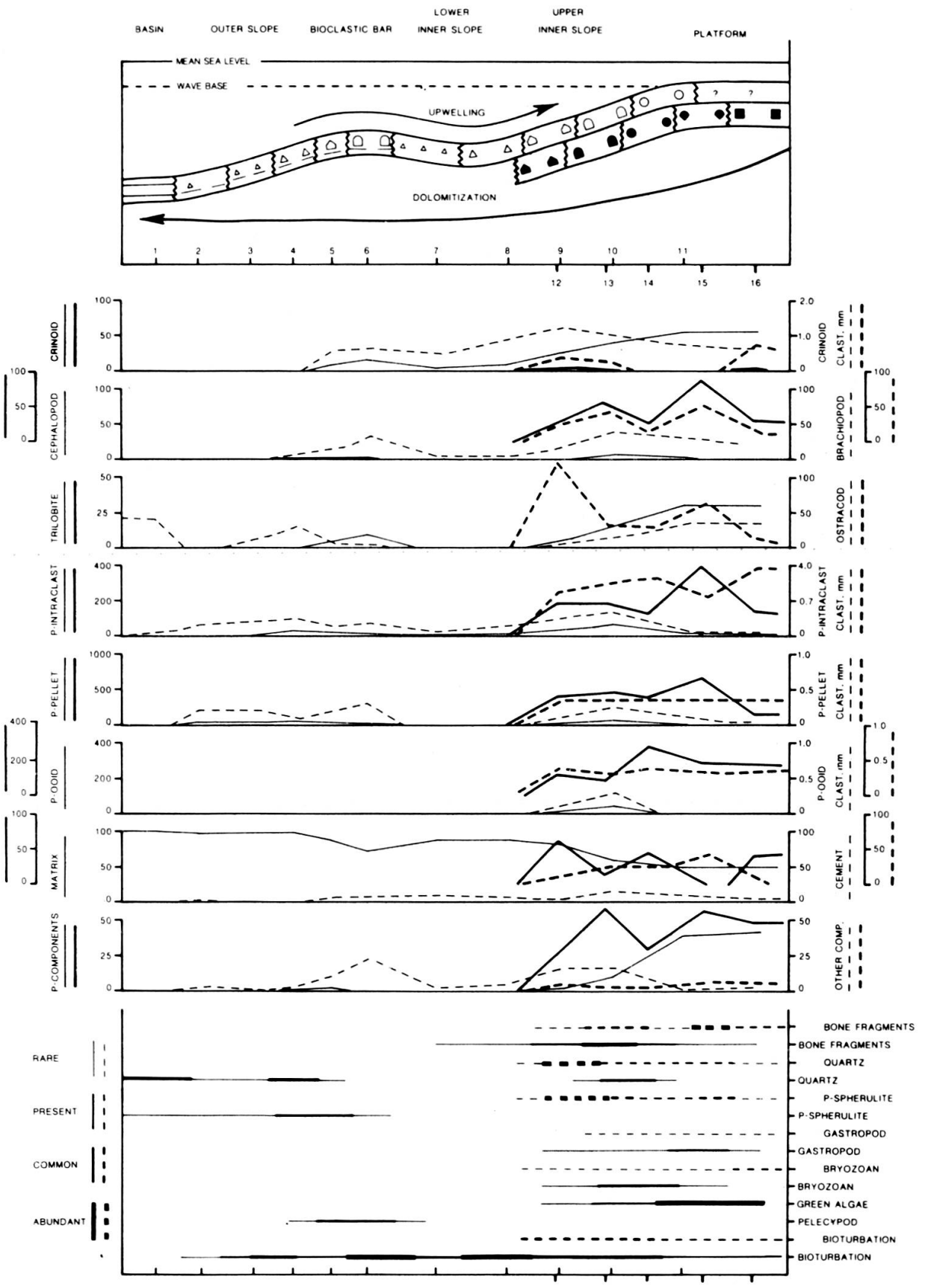

FIG. 7.

Ideal depositional model *(continued)*.

of the proposed model. Increased cement, decreased matrix and their irregular behavior in microfacies 12 through 16 are characteristic of the higher energy synsedimentary phosphatization processes over the platform. Similar conclusions can be reached by observing variation of curves of all other non-phosphatic components versus the phosphatic ones.

Crystallinity of dolomite (expressed by the maximum dolomite rhomb size) reflects the grain size of the original replaced carbonate as observed in other instances, and hence bears a direct relationship to the energy curve of the environment of deposition (Okhravi and Carozzi, 1983).

Variations in mineralogic data lead to a refinement of the petrographic characteristics of microfacies determination and provide further insight into the physico-chemical conditions of the environments of deposition. Carbonate percent increases steadily toward the platform recording increased carbonate precipitation in more aerated and shallower conditions. However, carbonate percent decreases in microfacies 12 through 16 due to its replacement by apatite expressing penecontemporaneous phosphatization. The extrabasinal sediment yield of fine-grained detrital quartz, feldspar, and clay minerals gradually increases in frequency seaward corresponding to deposition of deeper water argillaceous microfacies which are clearly different from those of the greater energy platform where such small grain-size constituents were winnowed. Pyrite percent increases basinward indicating variation in reducing conditions and related accumulation of organic matter. The larger pyrite content in microfacies 12 through 16 is reflective of the conditions leading to precipitation of apatite on carbonate slope and platform: low dissolved oxygen, decrease in pH, high biological productivity, and a rapid accumulation of organic matter.

Total calcium (expressed in ppm) varies in agreement with the total carbonate content of the microfacies. The larger values in microfacies 12 through 16 are due to the large amount of Ca within the fluorapatite structure. The magnesium content (expressed in ppm) is representative of the amount of dolomite present. It shows a trend parallel to the carbonate percent, and roughly parallel to total calcium. The lesser magnesium values in microfacies 12 through 16 are due not only to the corresponding larger Ca and P values, but possibly also to an actual decrease in the chemical activity of magnesium during deposition because this element is considered an inhibitor to precipitation of marine apatites. The curve of iron follows the curve of pyrite percent for all microfacies.

The strontium content (expressed in ppm) is relatively small and its depletion is known to be an effect of dolomitization. Little variation occurs from microfacies 1 through 11, but strontium generally follows the same trend as calcium due to its substitution for Ca in calcite. The concentrations of Sr in microfacies 12 through 16 are significantly larger because strontium commonly is fixed in the fluorapatite lattice. The Sr/Ca ratio follows the same trend as Sr except for a significant increase

in microfacies 1 which may result from possible absorption of strontium on clay minerals. Total phosphorus is small (generally less than 10,000 ppm) in microfacies 1 through 11, it markedly increases in microfacies 12 to 16 due to precipitation of fluorapatite. The curve, therefore, is parallel to percent apatite. The Ca/Mg ratio is more useful as an indicator of changes in carbonate chemistry than Ca or Mg alone because it is independent of the actual percent carbonate present (calcite or dolomite). For microfacies 1 through 11, the Ca/Mg ratio is fairly constant. The increase in microfacies 10, and in 12 through 16 results from the increase in calcium associated with precipitation of fluorapatite. In addition, the presence of Mg ions in solution acts as an inhibitor to the precipitation of apatite and thus some of the negative correlation between P and Mg is probably due to a decrease in the activity of Mg in interstitial solutions.

The Fe/Mg curve follows a similar trend to that of percent pyrite and ppm iron. The large fluctuations in the Fe/Mg ratio for microfacies 12 to 16 are due to corresponding variations in Mg and Fe content which are magnified through the use of ratios and do not appear to be the result of any significant environmental fluctuations.

DIAGENESIS

Petrographic studies revealed two distinct periods of diagenesis: an early or penecontemporaneous phase, and a later one. The early phase is characterized by apatite replacement of micrite and calcisiltite, contemporaneous precipitation of pyrite, and minor amount of silicification through growth of authigenic crystals and replacement of bioclasts. Subsequent diagenesis involves formation of evaporites, calcite cementation, and dolomitization.

Phosphatization

Phosphatization occurred as a penecontemporaneous to early diagenetic replacement of calcium carbonate in the upper slope and platform environments. In microfacies 12 through 16 this is expressed by the abundance of phosphatized bioclasts (Plate 3A, B, C), and formation of structureless nodules (Plate 3D) containing varied phosphatic grains and bioclasts while penecontemporaneous reworking by currents produced ooids, structureless lithic pellets and intraclasts (Plate 3E). Early apatite replacement of calcisiltite matrix also occurs, within burrows or patchy microenvironments conducive to apatite precipitation, in microfacies 8 and 10. In these microfacies, the finer-grained calcite is completely replaced, while the larger grains and bioclasts are marginally replaced.

Identification of clay minerals was undertaken to determine a possible relationship between the precipitation of apatite and the clay mineral species present. There

was little variation, however, in clay minerals between microfacies. For the most part, the clays are characterized by a predominance of discrete illite with varying amounts of heterogeneous mixed-layer illite-smectite and traces to moderate amounts of chlorite (which vary in Fe and Mg content from sample to sample, but are not microfacies controlled).

Pyritization

Petrographically, it is not possible to determine a time sequence between phosphate and pyrite. Pyritization of calcareous shales in which the bioclasts are filled with phosphalutite is common. Pyrite replacement of bioclasts can also be less specific and often more extensive (Plate 3B, C). Pyrite nodules (Plate 3F, G) are present in microfacies 13, 14, 15, and 16, and appear to have followed (slightly) the

---

PLATE 3.

Diagenetic features of Maquoketa phosphorites.

Phosphatization

A. Microfacies 16: Dolomitized intraphospharudite with an oolitic pelphospharenite matrix. As with most bioclasts, gastropod (center) is replaced by apatite. Ostracods (lower right) have been replaced by silica, but are filled with phosphalutite.

B. Microfacies 14: Dolomitized intraclastic pelphospharenite with argillaceous calcisiltite matrix. Well-preserved fenestrate bryozoan is replaced by apatite and pyrite. Apatite replacement of groundmass leads to nodular aspect.

C. Microfacies 15: Dolomitized grain-supported to pressure-welded intraclastic pelphospharenite with sparite cement. Silicified ostracod (center) is filled with phosphalutite. Orthocone cephalopod (center) is also replaced by apatite. Many phosphatic bioclasts and grains are marginally to completely replaced by pyrite.

D. Microfacies 14: Dolomitized intraclastic pelletoidal oophospharenite. Large phosphatic nodule contains phosphatic ooids, lithic pellets, and intraclasts. The ooids and pellets within the nodule are uncompacted indicating its penecontemporaneous development.

E. Microfacies 10: Phosphatic biocalcarenite with a large phosphatic intraclast. Intraclast has been bored indicating derivation from a hardground surface.

Pyritization

F. Microfacies 16: Dolomitized intraphospharudite with pelletoidal oophospharenite matrix. Dolosparite cement (right) is patchy. Pyrite replacement of matrix and grains produced massive nodule (left).

G. Microfacies 13: Dolomitized grain-supported intraclastic pelphospharenite. Articulated silicified ostracods are well-preserved. Pyrite has developed a micronodular aspect.

Evaporites

H. Microfacies 12: Dolomitized intraclastic pelphospharenite with an argillaceous calcisiltite matrix. The latter has been brecciated by development of selenite gypsum, later replaced by a pseudomorphic calcite cement.

All photomicrographs: plane-polarized light.

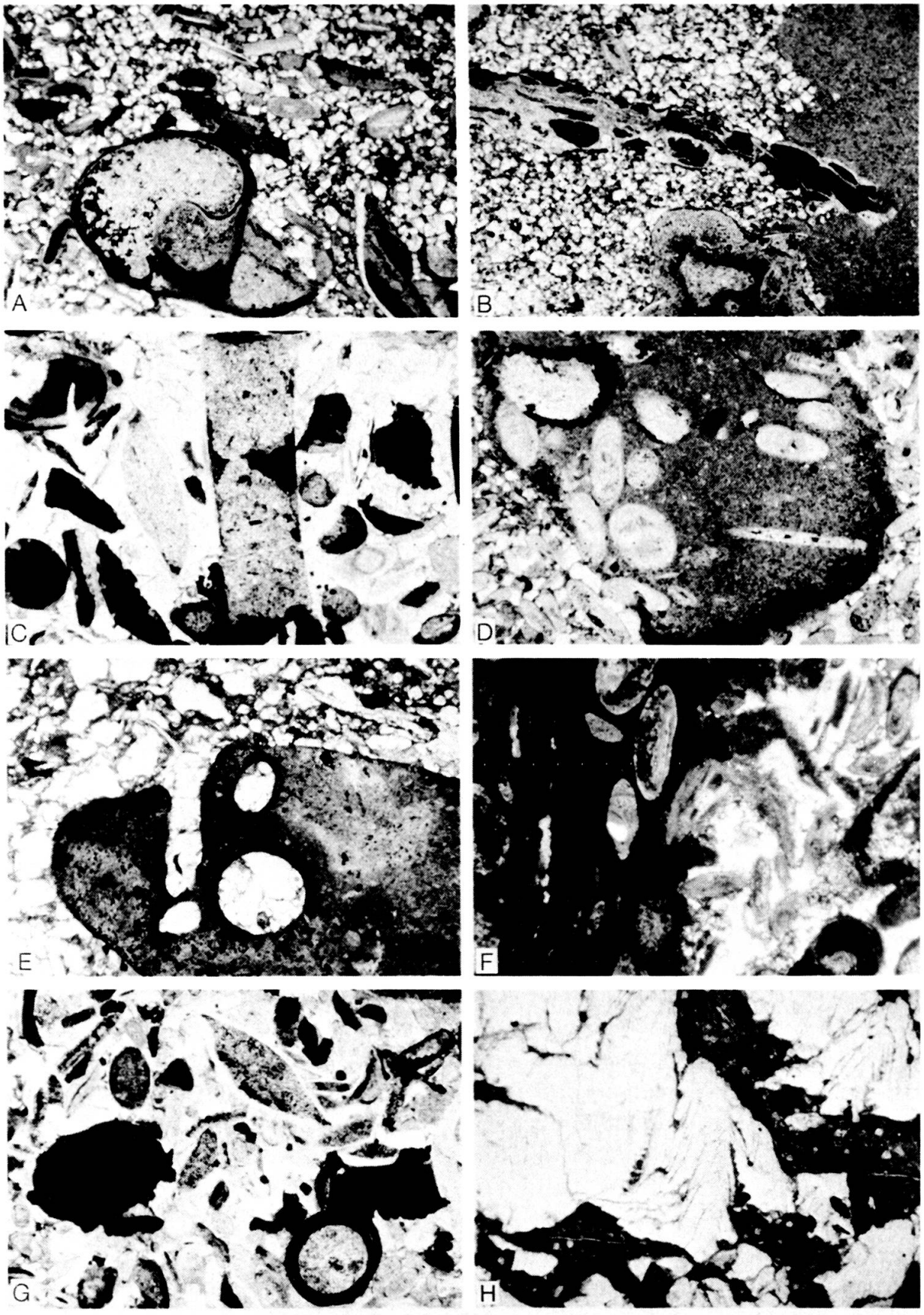
A
B
C
D
E
F
G
H
0.5mm

formation of phosphatic ooids and pellets, which are, in places, surrounded by nodular pyrite. Disseminated pyrite is also a common feature of all phosphatic microfacies. The conditions which have allowed for precipitation of phosphate, are also conducive to the formation of pyrite. In particular, the influx of organic and nutrient-rich water onto the carbonate platform produces an environment in which early diagenesis of organic-rich, anoxic sediments forms pyrite. The association of pyrite and apatite has been observed in phosphorites globally (Kolodny, 1980).

Silicification

Silicification is relatively minor in comparison with phosphatization and pyritization. Silicification is present as a marginal to complete replacement of bioclasts, in particular brachiopod and crinoid fragments, and ostracods (Plate 3C, G). A few minor patches of microcrystalline quartz are also present in microfacies 12 through 16. The timing of silicification compared to dolomitization is shown by euhedral dolomite rhombs cross cutting silicified bioclasts. No clear time relationship to phosphatization or pyritization, however, has been determined. Articulated silicified ostracods are usually found filled with phosphalutite (Plate 3C, G), and silicified bioclasts are marginally replaced by apatite. In addition, authigenic quartz and feldspar laths are observed to cut across margins of phosphatic intraclasts and nodules and to crystallize within them, indicating the close relationship of phosphatization and silicification. The association of phosphorus and silica, along with carbon, has been recognized as an association of elements related to biological activity (Kolodny, 1980) which is a factor in the formation of phosphorites, cherts, and organic matter-rich shales. Upwelling of nutrient rich, oxygen-poor waters onto the carbonate slope, not only provides an additional source of phosphorus, but is likely the source for the silica necessary for the silicification observed.

Evaporite Precipitation

Evaporite precipitation is indicated by the presence of calcite pseudomorphs after chickenwire anhydrite and selenite gypsum (Plate 3H). Precipitation of gypsum followed early diagenetic phosphate and pyrite, as indicated by the brecciation of the calcisiltite matrix in microfacies 12 and 13, but the relationship to cementation and dolomitization remains unclear. Thin beds of chickenwire anhydrite (microfacies 1A) are interbedded with bituminous shales (microfacies 1) in the Missouri core DC and no evidence exists for a break in sedimentation between the two microfacies. The lowest evaporite bed is directly on top of the hardground in microfacies 13, and the fracturation by selenite gypsum in that microfacies is probably related. Although the presence of evaporite textures is only observed in the Missouri core DC, traces of gypsum were found (through X-ray diffraction) in samples from the other cores, and are associated with microfacies 12 through 16. A postdepositional precipitation

of gypsum and anhydrite, following phosphatization, mostly in the basinal microfacies has to be considered as the result of local restricted conditions which remain to be explained due to the lack of other control points. Later replacement is shown by the occurrence of calcite pseudomorphs (Plate 3H).

Cementation

Cementation is characterized by dolosparite-filled cavities and interparticle pores. The dolomite is considered to have retained the original texture of the calcite it has replaced (in this case sparite cement). Although dolomitized, it was observed that a drusy rim cement developed along the walls of vugs and borings and was overlain by a blocky sparite cement. This cementation is interpreted as saturated

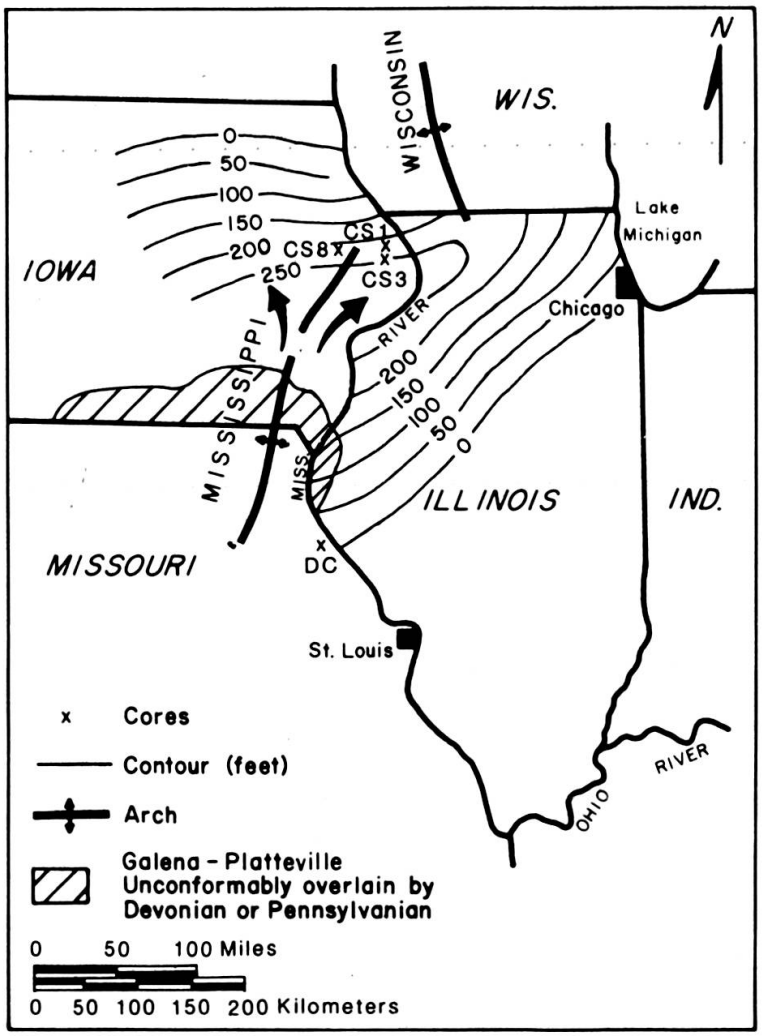

FIG. 8.

Isopach map of dolomite of Galena Group. Arrows around Mississippi River Arch are the possible pathways of circulation of mixed marine freshwater of the dorag system of dolomitization (modified from Bakush and Carozzi, 1986).

freshwater phreatic in origin. Pseudomorphic calcite cement after gypsum and anhydrite is also present as indicated above.

Dolomitization

Petrographically, dolomitization is characterized by a partial to complete replacement of bioclasts (Plate 1E, F, H; Plate 2A, C), replacement of micrite and calcisiltite matrix (Plate 1C, D, G, H), development of a dolosparite interparticle and cavity-filling cement which replaced original calcite varieties, and overgrowths on carbonate bioclasts and grains (Plate 2B to H). The timing relationship of dolomite to apatite precipitation is clearly indicated by the presence of euhedral dolomite rhombs within a phosphalutite matrix, and marginal replacement by dolomite of phosphatic intraclasts, nodules, lithic pellets and ooids.

The widespread dolomitization of Ordovician carbonates in the investigated area can be explained by the development of a dorag-type mixing zone in structurally positive areas at the time of worldwide glacio-eustatic fall in sea level at the end of the Ordovician. Bakush and Carozzi (1986) suggested that a paleostructural high corresponding to the most extensive dolomitization in the Galena Group could solve the paleohydrologic problems (Figure 8). Indeed, the three cores from Iowa which are completely dolomitized fall within the thickest part of the Galena and correspond to the area of most extensive dolomitization. The core from Missouri, which is partly dolomitized in the Maquoketa and not in the Galena, is located along the flanks of that same paleohigh.

REGIONAL PALEOGEOGRAPHY

During the late Ordovician (Edenian-Maysvillian) the investigated area was a slope environment at approximately 20° south latitude connecting a shallow equatorial platform in the northwest to a basinal area in the southeast which was bordered by the Taconic uplands located at 30° latitude south. In a paleoclimatic viewpoint, these conditions corresponded to a high pressure zone at 30°S with a low pressure zone at the Equator and trade winds blowing from the southeast. This would set up an anticlockwise offshore advection from the Ouachita continental margins producing upwelling of cold nutrient-rich waters onto a warm carbonate shelf and considered responsible for the formation of the basal Maquoketa phosphorites.

It is quite possible that the position of the Taconic landmass may have produced monsoonal perturbations of this system depending on the area and the latitudinal extent of the landmass. At any rate, the circulation pattern would be strengthened during a winter monsoon with increased high pressure over the Taconics resulting in enhanced southeast trade wind flow moving water offshore, and probably deepen-

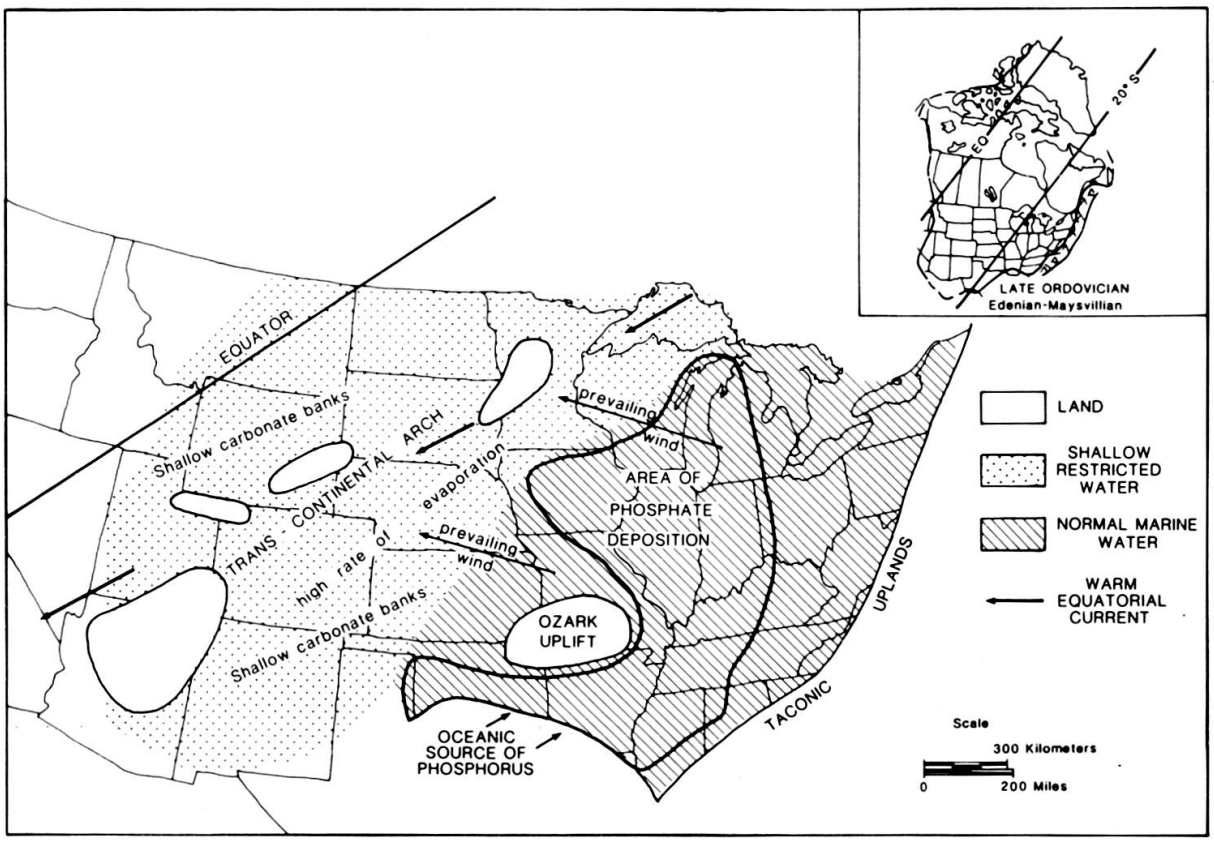

FIG. 9.

Generalized paleogeographic map of the Upper Ordovician in the central United States, showing major structural features, general wind and current direction, and generalized distribution of paleoenvironments. Normal marine waters existed in the eastern half of the continent whereas more restricted shallow-water environments were present in the west. The heavy black line outlines the general region of phosphate deposition during lower Maquoketa-Maysvillian time resulting from an anticlockwise upwelling under a quasi-geostrophic open ocean model. Modified from Ross (1976) and Witzke (1980).

ing the depth of upwelling. This winter deepening of the source of upwelling might favor phosphatization of carbonate sediments as the phytoplankton would be relatively dormant due to lower light levels, and thus would not be competing for phosphorus. During the summer, the 30° latitude high would weaken, however as the landmass is subtropical, the pressure contrast would be maintained so that trade winds would not reverse thus stopping the upwelling. This non-reversal implies that the Taconics and associated landmasses did not extend to any great degree into the temperate latitudes, which is in agreement with Ordovician paleogeographic reconstructions of Laurentia. In summary the proposed mechanism of upwelling belongs to a simple quasi-geostrophic open ocean model of Sverdrup-Ekman type (Stommel, 1957).

It is clear from the cyclicity of the lower Maquoketa sediments (bituminous shales interbedded with argillaceous carbonates and phosphatized carbonates) that repeated

glacio-eustatic fluctuations of sea level expressing the late Ordovician glaciation (Berry and Boucot, 1973) complicated the oceanographic model suggested above. Further local fluctuations of depositional environments can be attributed to periodic uplifts and downwarps along the Transcontinental Arch and the Ozark Uplift.

CONCLUSIONS

This study of the basal Maquoketa phosphorites shows that a terminology similar to that of carbonate rocks and based on the grain-size of the principal phosphate fraction and the nature of the matrix or cement is indispensable for an adequate description and interpretation of these complex rocks. Furthermore, a precise definition of phosphorite microfacies requires that petrographic and textural data be combined with mineralogic determinations of the amounts of calcite, dolomite, apatite, clay minerals, feldspars, quartz, and pyrite, and with geochemical determinations of the contents of Ca, Mg, Sr, Fe, and P.

As a result of this combined approach, an assumed simple sequence of phosphorites and associated carbonates and shales was found to consist of 16 distinct microfacies which build a carbonate-phosphorite depositional model extending from basinal conditions through slope into a platform environment.

The vertical succession of these microfacies indicates a complex cyclicity including two episodes of upwelling and related synsedimentary phosphatization, pyritization, and silicification of upper inner slope and platform carbonates. These conditions are accounted by a simple quasi-geostrophic open ocean model further complicated by glacio-eustatic fluctuations of sea level expressing the late Ordovician glaciation, and local tectonic activity.

REFERENCES

BAKUSH, S. H., and A. V. CAROZZI (1986). Subtidal storm-influenced carbonate ramp model: Galena Group (Middle Ordovician) along Mississippi River (Iowa, Wisconsin, Illinois, and Missouri), USA: *Archives des Sciences, Genève,* 39, 2,141-183.

BERRY, W. B. N., and A. J. BOUCOT (1973). Glacio-eustatic control of Late Ordovician-Early Silurian platform sedimentation and faunal changes: *Geol. Soc. America Bull.,* 84, 1, 275-284.

BLACK, N. R. (1985). Petrography and diagenesis of the Galena (Middle Ordovician) — Maquoketa (Late Ordovician) contact and the basal Maquoketa phosphorites in Eastern Missouri and Eastern Iowa, USA, *Unpubl. MS thesis, Department of Geology, University of Illinois (Urbana-Champaign),* 133p.

BRETSKY, P. W., and J. J. BERMINGHAM (1970). Ecology of the Paleozoic scaphopod genus *Plagioglypta* with special reference to the Ordovician of eastern Iowa: *Jour. Paleo.*, 44, 5, 908-924.

BROWN, C. E. (1974). Phosphatic zone in the lower part of the Maquoketa shale in northeastern Iowa: *US Geol. Surv. Jour. Research,* 2, 219-232.

KOLATA, D. R., and A. M. GRAESE (1983). Lithostratigraphy and depositional environments of the Maquoketa Group (Ordovician) in northern Illinois: *Illinois Geol. Survey Circular 528,* 49 p.

KOLODNY, Y. (1980). The origin of phosphorite deposits in the light of occurrences of Recent sea-floor phosphorites (extended abs.), *in* BENTOR, Y. K. (ed.), Marine phosphorites, geochemistry, occurrence, genesis: *Soc. Econ. Paleo. Min., Special Publ. No. 29,* 249.

LADD, H. S. (1925). Depauperate fauna of the Maquoketa Group (abs.): *Geol. Soc. America Bull., 36,* 228.

OKHRAVI, and A. V. CAROZZI (1983). The Joachim Dolomite: a middle Ordovician sabkha of southeastern Missouri, and southern Illinois, USA; *Archives des Sciences, Genève,* 36, 3, 373-424.

ROSS, R. J. (1976). Ordovician sedimentation in the western United States, *in* 1976 Symposium on Geology of the Cordilleran Hingeline: *Rocky Mountain Assoc. Geologists,* 109-133.

SLANSKY, M. (1980). Géologie des phosphates sédimentaires: *Bureau de Recherches géologiques et Minières, Paris, Mémoire No. 114,* 92 p.

SNYDER, J., and P. W. BRETSKY (1971). Life habits of diminutive bivalve mollusks in the Maquoketa Formation (Upper Ordovician): *Amer. Jour. Science,* 271, 3, 227-251.

STOMMEL, H. M. (1957). A survey of ocean current theory: *Deep-Sea Research,* 4, 1, 149-184.

WITZKE, B. J. (1980). Middle and Upper Ordovician paleogeography of the region bordering the Transcontinental Arch, *in* FOUCH, T. D., and E. R. MAGATHAN (eds.), Paleogeography of the west-central United States: *Soc. Econ. Paleo. Min., Rocky Mountain Section, Denver, Colorado,* 1-18.

—— (1983). Ordovician Galena Group in Iowa subsurface, *in* DELGADO, D. J. (ed.), Ordovician Galena Group of the Upper Mississippi Valley — Deposition, diagenesis, and paleoecology: *Guidebook for the 13th Annual Field Conference, Great Lakes Section Soc. Econ. Paleo. Min., Sept. 30-Oct. 2, 1983,* D1-D26.